

Matching Hagedorn mass spectrum with Lattice QCD

Pok Man Lo,¹ Michał Marczenko,¹ Krzysztof Redlich,^{1,2} and Chihiro Sasaki^{1,3}

¹*Institute of Theoretical Physics, University of Wrocław, PL-50204 Wrocław, Poland*

²*Extreme Matter Institute EMMI, GSI, Planckstrasse 1, D-64291 Darmstadt, Germany*

³*Frankfurt Institute for Advanced Studies, D-60438 Frankfurt am Main, Germany*

(Dated: July 22, 2022)

Based on recent Lattice QCD (LQCD) results obtained at finite temperature, we discuss modeling of the hadronic phase of QCD in the framework of Hadron Resonance Gas (HRG) with discrete and continuous mass spectra. We focus on fluctuations of conserved charges, and show how a common limiting temperature can be used to constrain the Hagedorn exponential mass spectrum in different sectors of quantum number, through a matching of HRG and LQCD. For strange baryons, the extracted spectra are found to be consistent with all known and expected states listed by the Particle Data Group (PDG). The strange-mesonic sector, however, requires additional states in the intermediate mass range beyond that embodied in the database.

PACS numbers: 12.40.Yx, 12.40.Nn, 14.20.Jn, 14.40.Df

I. INTRODUCTION

The thermodynamics of the confined phase of QCD is commonly modeled with the Hadron Resonance Gas (HRG) [1–8]. The equation of state for strongly interacting matter at finite temperature is well described by this model, formulated with a discrete mass spectrum of the experimentally confirmed particles and resonances. This finding was verified by recent results of Lattice QCD (LQCD) [9–12]. However, LQCD also reveals that, when considering fluctuations and correlations of conserved charges, there are clear limitations in the HRG description [11]. This is particularly evident in the strange sector, where the second order correlations with the net-baryon number χ_{BS} or strangeness fluctuations χ_{SS} are larger in LQCD than those in the HRG model [10, 11]. Such deviations were attributed to the missing resonances in the Particle Data Group (PDG) database [11].

Different extensions of the HRG model have been proposed to quantify the LQCD equation of state. They account for a possible repulsive interaction among constituents and/or a continuously growing exponential mass spectrum [5, 8, 13, 14]. The latter was first introduced by Rolf Hagedorn [15] within the Statistical Bootstrap model (SBM) [16–18], and was then studied in dual string and bag models [19–21]. For large masses, the Hagedorn spectrum $\rho(m)$ is parametrized as $\rho(m) \simeq m^a e^{m/T_H}$, where T_H is the Hagedorn limiting temperature and a is a model parameter.

The main objective of this paper is to analyze LQCD data on fluctuations and correlations of conserved charges within the HRG model. In particular, we examine whether the missing resonances contained in the asymptotic Hagedorn mass spectrum are sufficient to quantify LQCD results. We focus on the susceptibilities χ_{BS} and χ_{SS} , where LQCD indicates the largest deviations from HRG, in spite of their agreement on the equation of state in the hadronic phase.

To calculate fluctuations of conserved charges within

HRG, one needs to identify the hadron mass spectrum for different quantum numbers. For a continuous mass spectrum $\rho(m)$, this issue was addressed in Refs. [22] and [23], where the parameters of $\rho(m)$ in different hadronic sectors were extracted by fitting the spectra to the established hadronic states in the PDG database [24]. It was shown in Ref. [23] that the Hagedorn temperatures for mesons T_H^M and baryons T_H^B are different, with $T_H^M > T_H^B$. The $T_H^B \simeq 140$ MeV found in [22] is clearly below the LQCD crossover temperature $T_c = 155(1)(8)$ MeV from hadronic to quark-gluon plasma phase [25–27]. This, however, is inconsistent with LQCD, as it implies a large fluctuation of the net-baryon number deep in the hadronic phase, which is not observed in lattice simulations.

In this study we have reanalyzed the Hagedorn mass spectrum in different sectors of quantum number, in the context of the PDG data, and have shown that there is a common Hagedorn temperature for mesons and baryons in different strange sectors. We have applied our newly calculated $\rho(m)$ in the HRG model to explore different thermodynamics observables, in particular, fluctuations of conserved charges. The results are compared with LQCD for the strangeness, net-baryon number fluctuations, and for baryon-strangeness correlations. We show that HRG, adopting a continuous mass spectrum with its parameters fitted to the PDG data, can partially account for the missing resonances needed to quantify LQCD results.

To fully identify the missing resonance states, we motivate a matching of LQCD and HRG to extract a continuous mass spectrum $\rho(m)$. In the strange-baryonic sector, this $\rho(m)$ is shown to be consistent with all known and expected states listed by the PDG. However, the mass spectrum for strange mesons require some additional resonances in the intermediate mass range beyond those listed in the PDG compilation.

The paper is organized as follows: In Sec. II, we introduce the HRG thermodynamics with a discrete mass spectrum. In Sec. III, we discuss HRG model compar-

isons with LQCD. In Sec. IV, we extract the continuous $\rho(m)$ in different sectors of quantum number and discuss fluctuations of conserved charges in conjunction with LQCD findings. Finally, Sec. V is devoted to summary and conclusions.

II. EQUATION OF STATE OF HADRONIC MATTER

To formulate a phenomenological model of hadronic matter at finite temperature and density, one needs to identify the relevant degrees of freedom and their interactions. In the confined phase of QCD the medium is composed of hadrons and resonances.

The HRG model, in its simplest form, treats the medium constituents as point-like and independent [1]. Thus, in such a model setup, the interactions of hadrons and the resulting widths of resonances are neglected. Hence, the composition of the medium and its properties emerge through a discrete mass spectrum

$$\rho^{\text{HRG}}(m) = \sum_i d_i \delta(m - m_i), \quad (1)$$

where $d_i = (2J_i + 1)$ is the spin degeneracy factor of a particle i with mass m_i and the sum is taken over all stable particles and resonances.

The mass spectrum in Eq. (1) can be identified experimentally or can be calculated within LQCD. In both cases our knowledge is far from complete. The LQCD can determine the masses of hadronic ground states and low-lying excited states with fairly high precision [28]. However, the higher excited states are still not well controlled in lattice calculations.

The spectrum of experimentally established hadrons, summarized by the PDG [24], accounts for all identified particles and resonances, i.e., confirmed mesons and baryons granted with a three- or four-star status, of masses up to $m_M \simeq 2.4 \text{ GeV}$ and $m_B \simeq 2.6 \text{ GeV}$ respectively. The investigation of higher excited states remains a significant challenge for the experiments due to the complicated decay properties and large widths of the resonances.

Instead of the hadron mass spectrum (1), the medium composition can be characterized by the cumulant [22]

$$N^{\text{HRG}}(m) = \sum_i d_i \theta(m - m_i), \quad (2)$$

such that

$$\rho^{\text{HRG}} = \frac{\partial N^{\text{HRG}}}{\partial m}. \quad (3)$$

Thus, $N^{\text{HRG}}(m)$ counts the number of degrees of freedom with masses below m .

Since the spectrum (1) is additive in different particle species, it can be decomposed into a sum of contributions

from mesons and baryons, as well as a sum of particles with definite strangeness.

Fig. 1 shows the cumulants in different sectors of hadronic quantum number with inputs from the PDG. The cumulant of all hadrons is seen in Fig. 1(a) to rapidly increase with mass. For $m \leq 2 \text{ GeV}$ such increase is almost linear, indicating that the hadron mass spectrum is exponential, as predicted by Rolf Hagedorn in the context of SBM [15, 16].

A rapid increase in the number of states is also seen, in Figs. 1(b) and 1(c), to appear separately for the mesonic and baryonic sector, as well as for the strange and non-strange mesons with $m < 2 \text{ GeV}$. Baryons of different strangeness, as illustrated in Fig. 1(d), follow a similar trend with the exception of $|S| = 3$ baryons, which consists only of Ω hyperons.

For an uncorrelated gas of particles (and antiparticles) with a mass spectrum $\rho(m)$, the thermodynamic pressure $\hat{P} = P/T^4$ is obtained as

$$\hat{P}(T, V, \vec{\mu}) = \pm \int dm \rho(m) \int \frac{d\hat{p}}{2\pi^2} \hat{p}^2 [\ln(1 \pm \lambda e^{-\hat{\epsilon}}) + \ln(1 \pm \lambda^{-1} e^{-\hat{\epsilon}})], \quad (4)$$

where $\hat{p} = p/T$, $\hat{m} = m/T$, $\hat{\epsilon} = \sqrt{\hat{p}^2 + \hat{m}^2}$ and (\pm) -sign refers to fermions and bosons respectively. For a particle of mass m , carrying baryon number B , strangeness S and electric charge Q , the fugacity λ reads

$$\lambda(T, \vec{\mu}) = \exp(B\hat{\mu}_B + S\hat{\mu}_S + Q\hat{\mu}_Q), \quad (5)$$

where $\hat{\mu} = \mu/T$. Expanding the logarithm and performing the momentum integration in Eq. (4) with the discrete mass spectrum ρ^{HRG} in Eq. (1), one obtains

$$\hat{P} = \sum_i \frac{d_i}{\pi^2} \sum_{k=1}^{\infty} \frac{(\pm 1)^{k+1}}{k^2} \hat{m}_i^2 K_2(k\hat{m}_i) \cosh[k(B_i\hat{\mu}_B + S_i\hat{\mu}_S + Q_i\hat{\mu}_Q)], \quad (6)$$

where the first sum over i includes contributions of all known hadron species and K_2 is the modified Bessel function. The upper and lower sign is for bosons and fermions respectively. The Boltzmann approximation corresponds to retaining only the first term in k -summation.

The thermodynamic pressure in Eq. (4), through the mass spectrum ρ , contains all the relevant information about the distribution of mass and quantum number of the medium. Thus, it allows for the study of different thermodynamic observables, including fluctuations of conserved charges.

Furthermore, one can turn this argument around, and study the implications on the composition of the medium from a given set of thermodynamic observables. In the coming sections, we shall examine this idea quantitatively with the aid of recent lattice data.

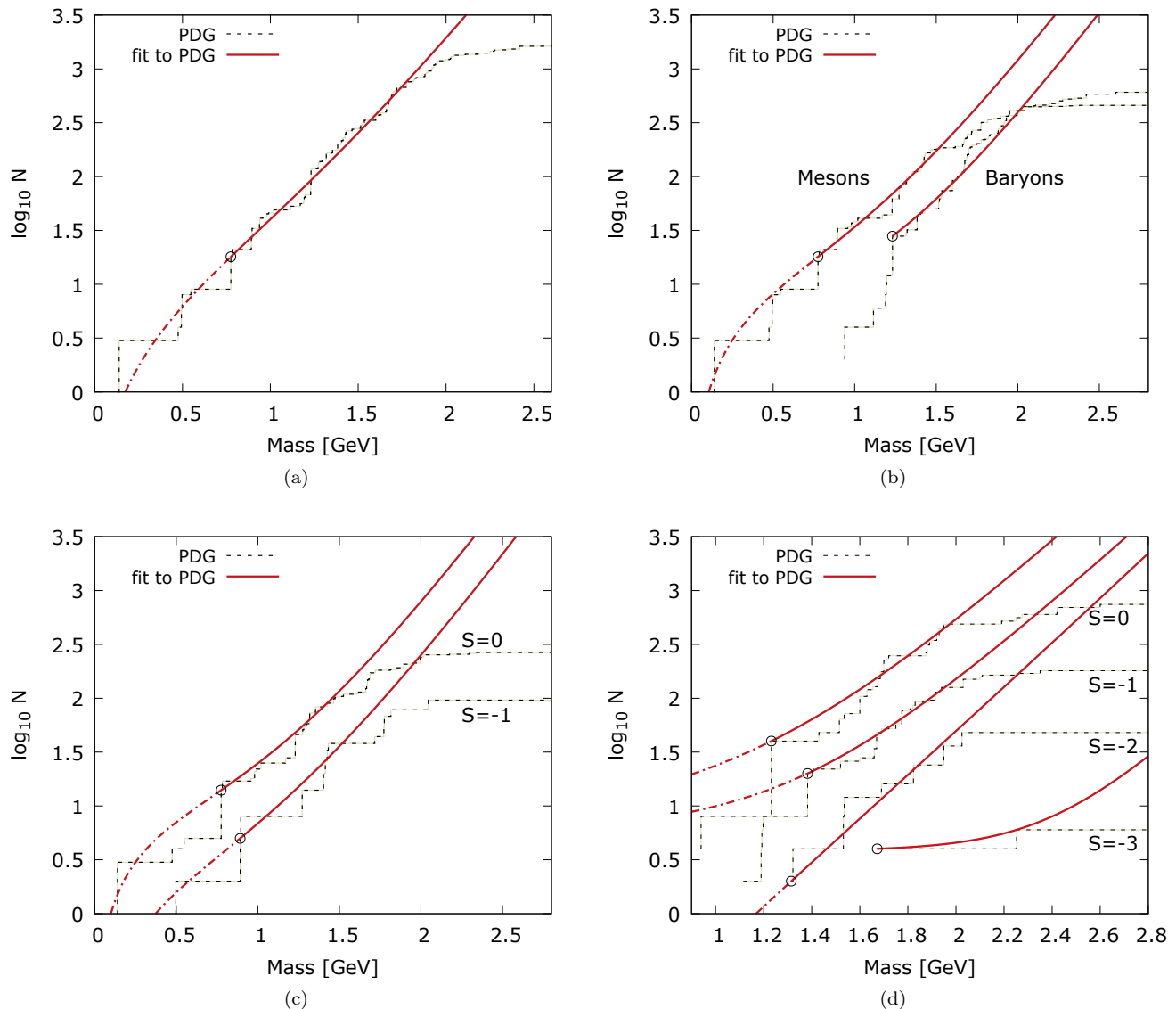


FIG. 1: (Color online) Cumulants of the PDG mass spectrum in different sectors of quantum number: (a) all hadrons; (b) mesons and baryons; (c) mesons of different strangeness; (d) baryons of different strangeness. The lines are obtained from the fit of Eqs. (9) and (11) to the PDG data with the parameters listed in Table I (see text).

III. HADRON RESONANCE GAS AND LQCD

LQCD provides a theoretical framework to calculate the equation of state and bulk properties of strongly interacting matter at finite temperature. The first comparison of the equation of state calculated on the lattice with that derived from Eq. (6) have shown, that thermodynamics of hadronic matter is well approximated by the HRG with mass spectrum generated on the corresponding lattice [2, 3].

At present we have more comprehensive information on the thermodynamics of hadronic matter from LQCD with physical quark masses and extrapolated to the continuum [12, 29, 30]. Thus, a direct comparison of the

equation of state from Eq. (4) and LQCD can be performed with the physical mass spectrum [4, 31, 32].

In Fig. 2(a) we show the temperature dependence of the thermodynamic pressure obtained recently in lattice simulations with physical quark masses [12, 29]. The bands of the LQCD result indicate the systematic errors due to continuum extrapolation. The vertical band marks the temperature $T_c = 155(1)(8)$ MeV, which is the chiral crossover temperature from the hadronic phase to the quark-gluon plasma [27]. These LQCD results are compared in Fig. 2(a) with predictions of the HRG model for the mass spectrum (1), which includes all known hadrons and resonances listed by the PDG [24].

There is a clear coincidence of the HRG and LQCD

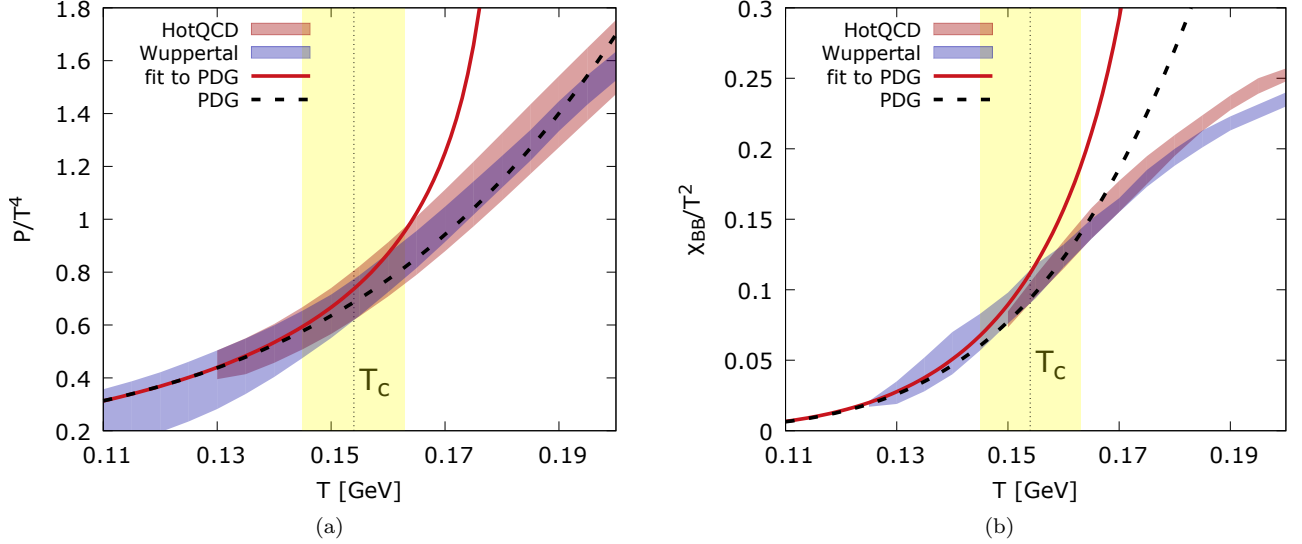


FIG. 2: (Color online) Lattice QCD results of HotQCD [29, 31] and Budapest-Wuppertal Collaboration (B-W Coll.) [9, 12] for different observables in dimensionless units: (a) the thermodynamic pressure; (b) the net-baryon number fluctuations χ_{BB} . Also shown are the HRG results for the discrete PDG mass spectrum (dashed line) with the continuous mass spectrum from Eq. (9) and with parameters fitted to the PDG (continuous line).

results on the equation of state at low temperatures. The pressure is strongly increasing with temperature towards the chiral crossover. This behavior is well understood within HRG as the consequence of growing contributions from the escalating number of higher resonances.

Although HRG formulated with a discrete mass spectrum does not exhibit any critical behavior, it nevertheless reproduces remarkably well the lattice results in the hadronic phase. This agreement has now been extended to the fluctuations and correlations of conserved charges [9, 10, 33, 34].

In a thermal medium, the second order fluctuations and correlations of conserved charges are quantified by the generalized susceptibilities

$$\hat{\chi}_{xy} = \frac{\partial^2 \hat{P}}{\partial \hat{\mu}_x \partial \hat{\mu}_y}, \quad (7)$$

where (x, y) are conserved charges, which in the following are restricted to the baryon number B and strangeness S .

For HRG with a discrete mass spectrum of Boltzmann particles, $\hat{\chi}_{xy}$ is obtained from Eq. (6) as

$$\hat{\chi}_{xy}^{\text{HRG}} \Big|_{\hat{\mu}_x=\hat{\mu}_y=0} = \frac{1}{\pi^2} \sum_i d_i \hat{m}_i^2 K_2(\hat{m}_i) x_i y_i. \quad (8)$$

The susceptibilities (7) and in particular (8) are observables sensitive to the quantum numbers of medium constituents. Thus, $\hat{\chi}_{xy}$ can be used to identify contributions of different particle species to QCD thermodynamics [33, 34].

Recent LQCD calculations of HotQCD Collaboration [10] and Budapest-Wuppertal Collaboration [9, 12]

provide results on different fluctuations and correlations of conserved charges. Thus, the apparent agreement of HRG and LQCD, seen on the level of the equation of state, can be further tested within different hadronic sectors [10].

In Figs. 2(b) and 3 we show the LQCD results on the fluctuation of net-baryon number, strangeness, as well as the baryon-strangeness correlations. They are compared to the HRG model, formulated with the PDG mass spectrum. From Fig. 2(b), it is clear that the net-baryon number fluctuation in the hadronic phase are well described by HRG, whereas strangeness fluctuation $\hat{\chi}_{SS}$ in Fig. 3(b) and $\hat{\chi}_{BS}$ correlation in Fig. 3(a) are underestimated in the low temperature phase.

Following an analysis of the relations between different susceptibilities of conserved charges, it was argued in Ref. [10] that deviations seen in Fig. 3(a) can be attributed to the missing resonances in the strange-baryonic sector. In view of Fig. 3(b), similar conclusion can be drawn for the strange mesons.

In general, the contributions of heavy resonances in HRG are suppressed due to the Boltzmann factor. However, the relative importance of these states depends on observable. In the hadronic phase, the pressure is dominated by the low-lying particles. At temperature $T = 150$ MeV, the contribution to the pressure from particles and resonances with mass $M > 1.5$ GeV is of the order of 7%. However, in the fluctuations of the net-baryon number and baryon-strangeness correlations, such contribution is already significant and amounts to 26% and 33%, respectively.

Contributions from missing heavy states could be the potential origin of the observed differences between

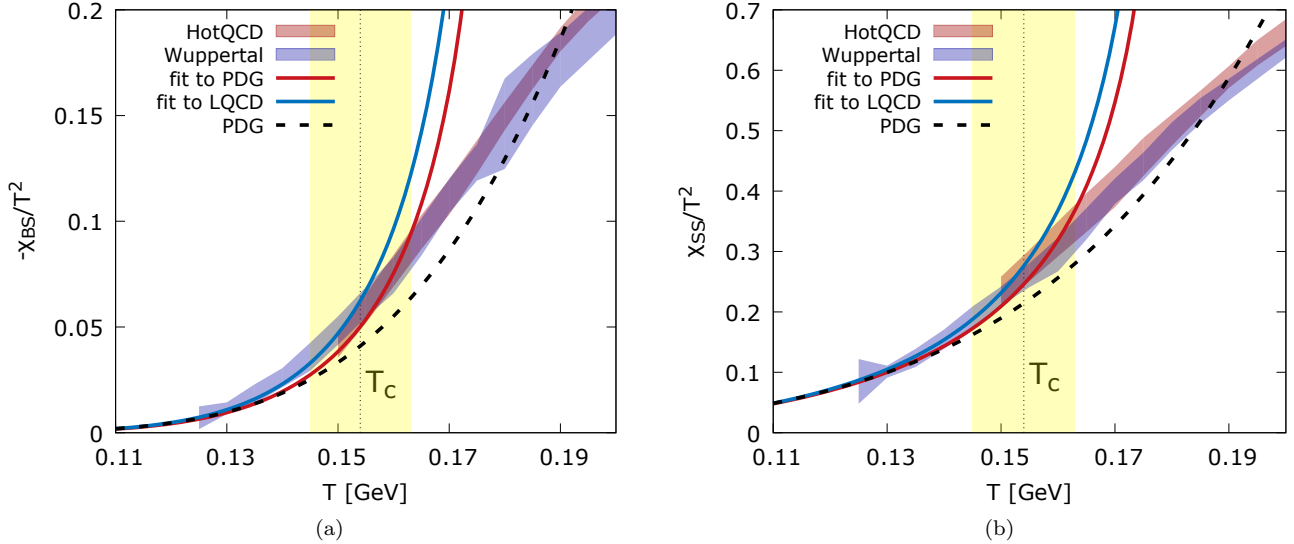


FIG. 3: (Color online) As in Fig. 2, but for baryon-strangeness correlations $\hat{\chi}_{BS}$, (a) and for strangeness fluctuations $\hat{\chi}_{SS}$ (b). Also shown are the corresponding results obtained from the least square fit to lattice data up to $T \simeq 156$ MeV.

LQCD results and HRG predictions on fluctuations and correlations of conserved charges in the strange sector, shown in Figs. 3(a) and 3(b).

IV. HAGEDORN MASS SPECTRUM AND LQCD FLUCTUATIONS

To account for the unknown resonance states at large masses we adopt the continuous Hagedorn mass spectrum with the following parametrization

$$\rho^H(m) = \frac{a_0}{(m^2 + m_0^2)^{5/4}} e^{m/T_H}, \quad (9)$$

and its corresponding cumulant

$$N^H(m) = \int_0^m dm' \rho^H(m'), \quad (10)$$

where T_H is the Hagedorn limiting temperature, whereas a_0 and m_0 are additional free parameters.

In general, the parameters of $\rho(m)$ can be calculated within a model, e.g., in SBM [16, 18]. In the following, we considered the Hagedorn temperature and the weight parameters (a_0, m_0) in Eq. (9) based on the mass spectrum of the PDG. In addition, we assume that the same exponential functional form holds separately for hadrons in different sectors of quantum number, i.e., for mesons and baryons with or without strangeness.

The analysis of experimental hadron spectrum, in the context of Hagedorn exponential form, has been extensively discussed in the literature [14, 16, 17, 35]. In one of the recent studies [22, 23], it was shown that in fitting the Hagedorn spectrum to experimental data, one arrives

at different limiting temperatures for mesons, baryons and hadrons with different electric charges. In particular, with $\rho(m)$ from Eq. (9), the limiting temperature for mesons, $T_H^M \simeq 195$ MeV, was extracted to be considerably larger than that for baryons, $T_H^B \simeq 140$ MeV. Such Hagedorn limiting temperatures, however, are inconsistent with recent lattice results, which show that the change from the hadronic to the quarks and gluons degrees of freedom in different sectors appear in the same narrow temperature range of the chiral crossover. Thus, the Hagedorn temperature of baryons should appear beyond the chiral crossover, i.e., $T_H^B > 155$ MeV. In addition, the LQCD data on $\hat{\chi}_{BB}$ are consistent with the discrete PDG baryon mass spectrum up to $T \simeq 160$ MeV. This seems to suggest that large contributions from heavy resonances are not expected in $\hat{\chi}_{BB}$ at $T_H^B < 155$ MeV.

From the above one concludes that it is very unlikely for the Hagedorn limiting temperatures in various hadronic sectors to differ substantially. Moreover, they are expected to be larger than the chiral crossover temperature. Consequently, the extracted Hagedorn temperature $T_H^B \simeq 140$ MeV for baryons in Ref. [22, 23], though mathematically correct, is disfavored by LQCD.

The reason for the very different Hagedorn temperatures for mesons and baryons, is that the extraction of the parameters in Eq. (9) has been performed over the whole mass range of the PDG data. The low-lying baryons are driving the fit towards a lower T_H , resulting in the deviation of Hagedorn temperatures among different sectors.

To avoid the above problem, we adopt Hagedorn's idea

to treat the contributions of ground state particles¹ separately from the exponential mass spectrum. In addition, we start the continuous part of the spectrum from the onset of the first resonance in the corresponding sector. Therefore, we apply the following form of the mass spectrum

$$\rho(m) = \sum_i d_i \delta(m - m_i) + \rho^H(m) \theta(m - m_x), \quad (11)$$

and the corresponding cumulant

$$N(m) = \sum_i d_i \theta(m - m_i) + \theta(m - m_x) \int_{m_x}^m dm \rho^H(m), \quad (12)$$

where $\rho^H(m)$ is given by Eq. (9). The index i counts the hadronic ground states, and x is the first resonance in the corresponding sector.

The above spectrum can now be compared with the experimental data listed by the PDG, in different sectors of quantum number. From the analysis of the mass spectrum parameters of all hadrons, we find that the best description is obtained with $T_H \simeq 180$ MeV. This value is consistent with that recently found in Ref. [14]. In addition, $T_H \simeq 180$ MeV is the largest temperature obtained as the solution of the Bootstrap equation [36]. In the following, we apply the same T_H for strange and non-strange hadrons.

In Fig. 1 we show that the spectra of PDG hadrons in different sectors are indeed properly described by the asymptotic mass spectrum (11) with a common Hagedorn temperature $T_H \simeq 180$ MeV. The weight parameters (a_0, m_0) in Eq. (9) are determined by the composition and decay properties of the resonances, hence, they are distinct for each hadronic quantum number. The optimal sets of parameters of $\rho(m)$ in Eq. (9) are summarized in Table I. The corresponding mass spectra are shown in Fig. 1 as continuous lines, whereas circles indicate the lowest masses m_x of the corresponding fit. Also shown, as broken lines in Fig. 1, are the extrapolated cumulants below m_x .

It is important for the decomposition of the hadron mass spectrum (11) into different sectors, using parameters from Table I, to produce results that are thermodynamically consistent. Thus, e.g., the total pressure \hat{P}^H obtained from Eq. (4) with the mass spectrum from Fig. 1(a), should be consistent with the sum of meson \hat{P}_M and baryon \hat{P}_B pressures, calculated with the mass spectra in Fig. 1(b). Similar results should hold for the pressure when adding up the contributions from strange particles in different sectors. This consistency check provides further constraints on the mass spectrum parameters presented in Table I.

	fit to PDG		fit to LQCD	
	a_0 [GeV ^{3/2}]	m_0 [GeV]	a_0 [GeV ^{3/2}]	m_0 [GeV]
ρ_H	0.75870	0.5379		
ρ_B	0.13606	0.1496		
ρ_M	0.43567	0.3240		
$\rho_B^{S=0}$	0.18553	0.1292		
$\rho_B^{S=-1}$	0.05032	0.0631	0.07944	0.3697
$\rho_B^{S=-2}$	0.03245	1.4011	0.05778	1.9603
$\rho_B^{S=-3}$	0.00027	0.00195		
$\rho_M^{S=0}$	0.28030	0.2611		
$\rho_M^{S=-1}$	0.09147	0.3432	0.11960	0.4656

TABLE I: The parameters of Hagedorn mass spectrum from Eqs. (9) and (11) obtained from the fit to the PDG data for: all hadrons ρ_H , all baryons ρ_B , all mesons ρ_M , baryons ρ_B^S and mesons ρ_M^S of different strangeness S . Also shown are the parameters obtained by matching LQCD results for second order fluctuations and correlations with the HRG model from Eq. (13) (see text). The Hagedorn temperature was fixed to $T_H = 180$ MeV.

With the PDG mass spectrum extrapolated to the continuum, we can now test whether heavy resonances can reduce or eliminate the discrepancies between HRG and LQCD on baryon-strangeness correlations and strangeness fluctuations, seen in Figs. 3(a) and 3(b).

The second order cumulants $\hat{\chi}_{xy}$, at vanishing chemical potential, are obtained in HRG as

$$\hat{\chi}_{BB}^H = \int_0^\infty \frac{dm}{\pi^2} \rho_B(m) \hat{m}^2 K_2(\hat{m}), \quad (13a)$$

$$\hat{\chi}_{SS}^H = \int_0^\infty \frac{dm}{\pi^2} \left[\rho_M^{S=-1}(m) + \sum_{k=1}^3 k^2 \rho_B^{S=-k}(m) \right] \hat{m}^2 K_2(\hat{m}), \quad (13b)$$

$$\hat{\chi}_{BS}^H = - \int_0^\infty \frac{dm}{\pi^2} \left[\sum_{k=1}^3 k \rho_B^{S=-k}(m) \right] \hat{m}^2 K_2(\hat{m}), \quad (13c)$$

using the mass spectrum $\rho(m)$ in Eq. (11) and the parameters presented in Table I.

In Figs. 2 and 3, we show the contribution of the continuous Hagedorn mass spectrum to the pressure and different charge susceptibilities. The results in Figs. 3(a) and 3(b) indicate that heavy resonances can capture, to a large extent, the differences between HRG and LQCD for strangeness and baryon-strangeness correlations. However, at low temperatures, $\hat{\chi}_{BS}$ still differs from the lattice. These deviations suggest that there are additional missing resonances in the PDG data in the mass range $m < 2$ GeV, as they begin to contribute substantially to $\hat{\chi}_{BS}$ and $\hat{\chi}_{SS}$ at lower temperatures.

To identify such low-lying state in the Hagedorn mass spectrum, one can use the LQCD susceptibility data as inputs for Eq. (13) to determine $\rho(m)$ in different sectors.

We have performed least square fits to LQCD data at $T < 156$ MeV to extract parameters of the mass spec-

¹ Particles that do not decay under strong interactions. In this context, there are no ground states in the $|S| = 2$ and $|S| = 3$ baryonic sectors.

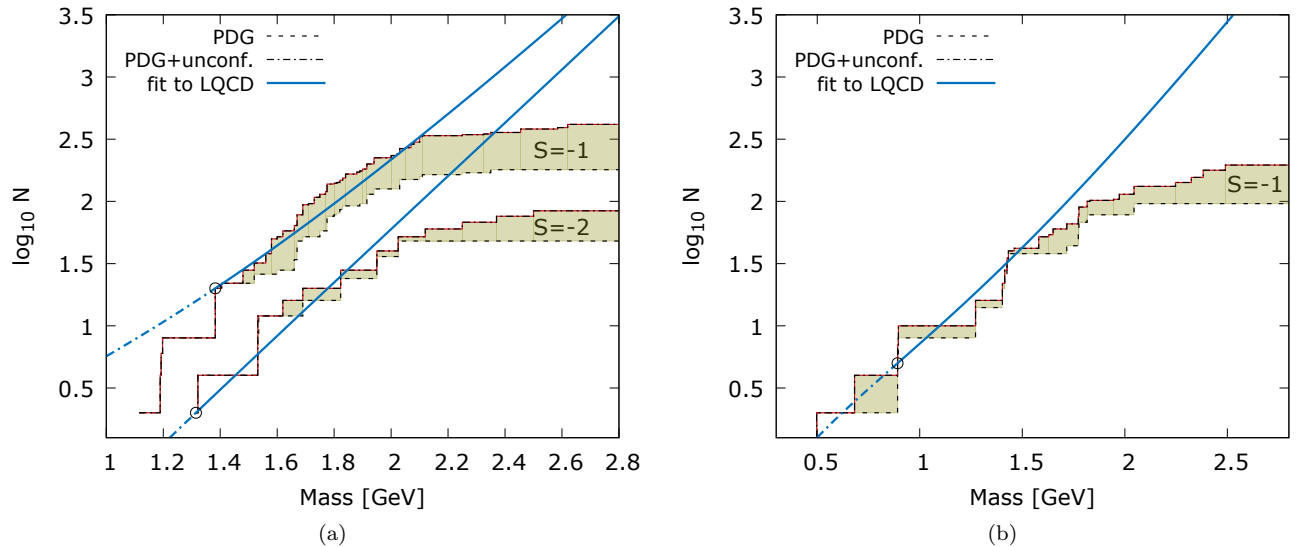


FIG. 4: (Color online) Cumulants of the PDG mass spectrum in different sectors of quantum number that includes only the confirmed states (broken line) and all states including those, which are expected but still not confirmed (broken-dashed line). The continuous lines are obtained by matching the LQCD results to the continuous mass spectrum (see text for details).

trum with a common $T_H \simeq 180$ MeV. The results are summarized in Table I. The susceptibilities $\hat{\chi}_{BS}$ and $\hat{\chi}_{SS}$ calculated with these parameters are shown in Fig. 3.

In Figs. 4(a) and 4(b) we show the cumulants of $\rho(m)$ obtained by matching LQCD with Eq. (13). Also shown in the figures are the experimental mass spectra including the unconfirmed states from the PDG. Most of the unconfirmed strange baryons are of $|S| = 1$. The contribution of these extra states to the cumulant is seen, in Fig. 4(a), to be fairly consistent with the optimal mass spectrum extracted from LQCD. This is also the case for the $|S| = 2$ baryons. The $|S| = 3$ sector is only weakly constrained by LQCD because of its negligible contribution to the second order susceptibilities. Therefore, we do not fit the corresponding parameters to the lattice.

In contrast to the strange-baryonic sector, the $|S| = 1$ meson spectrum extracted from LQCD, shown in Fig. 4(b), cannot be fully explained by the existing data of the PDG, even after the inclusion of the unconfirmed resonances. This may point to the existence of some uncharted strange mesons in the intermediate mass range.

V. SUMMARY AND CONCLUSIONS

Modeling the hadronic phase of QCD by the Hadron Resonance Gas (HRG), we have examined the contribution of heavy resonances, through the exponential Hagedorn mass spectrum $\rho(m) \simeq m^a e^{m/T_H}$, to the fluctuation of conserved charges. A quantitative comparison between model predictions and lattice QCD (LQCD) calculations is made, with a special focus on strangeness fluctuations and baryon-strangeness correlations.

We have reanalyzed the mass spectrum of all known hadrons and resonances listed in the Particle Data Group (PDG) database. A common Hagedorn temperature, $T_H \simeq 180$ MeV, is employed to describe hadron mass spectra in different sectors of quantum number. This value of T_H exceeds the LQCD chiral crossover temperature $T_c = 155(1)(8)$ MeV. The latter signifies the conversion of the hadronic medium into a quark-gluon plasma.

Applying the continuum-extended mass spectrum calculated from the PDG data, we have shown that the Hagedorn asymptotic states can partly remove the disparities with lattice results in the strange sector.

To fully identify the missing hadronic states, we perform a matching of LQCD data on strangeness fluctuations and baryon-strangeness correlations with HRG. The parameters of the Hagedorn mass spectrum $\rho(m)$ are well constrained by LQCD data in different sectors of strange quantum number, using the same limiting temperature $T_H \simeq 180$ MeV.

The mass spectra extracted from LQCD, for baryons with strangeness $|S| = 1, 2$, are shown to be consistent with the unconfirmed states in the PDG. This is not the case for the strange-mesonic sector, where the corresponding $\rho(m)$ exceeds the current data of the PDG, even after the unconfirmed states are included. This may point to the existence of some uncharted strange mesons in the intermediate mass range. Clearly, new data and further lattice studies are needed to clarify these issues. Moreover, such missing resonances could be of particular importance for modeling particle production yields in heavy ion collisions.

It would be interesting to assess the effects of resonance width on the Hagedorn spectrum. Recent studies suggest that the implementation of low-lying broad resonances

in thermal models must be handled with care [37, 38]. The impact on the global spectrum and consequently the thermodynamics is currently under investigation.

Acknowledgments

We acknowledge fruitful discussions with Bengt Friman. K. R. also acknowledges discussions with A.

Andronic, P. Braun-Munzinger, F. Karsch, J. Rafelski, H. Satz and J. Stachel. C. S. acknowledges partial support of the Hessian LOEWE initiative through the Helmholtz International Center for FAIR (HIC for FAIR). This work was partly supported by the Polish National Science Center (NCN), under Maestro grant DEC-2013/10/A/ST2/00106.

-
- [1] P. Braun-Munzinger, K. Redlich and J. Stachel, In *Hwa, R.C. (ed.) et al.: Quark gluon plasma* 491-599 (2003).
 - [2] F. Karsch, K. Redlich and A. Tawfik, Eur. Phys. J. C **29**, 549 (2003).
 - [3] F. Karsch, K. Redlich and A. Tawfik, Phys. Lett. B **571**, 67 (2003).
 - [4] F. Karsch, Acta Phys. Polon. Supp. **7**, no. 1, 117 (2014).
 - [5] A. Andronic, P. Braun-Munzinger, J. Stachel and M. Winn, Phys. Lett. B **718**, 80 (2012).
 - [6] M. Albright, J. Kapusta and C. Young, Phys. Rev. C **90**, no. 2, 024915 (2014).
 - [7] M. Albright, J. Kapusta and C. Young, arXiv:1506.03408 [nucl-th].
 - [8] V. Vovchenko, D. V. Anchishkin and M. I. Gorenstein, Phys. Rev. C **91**, no. 2, 024905 (2015).
 - [9] S. Borsanyi, Z. Fodor, S. D. Katz, S. Krieg, C. Ratti and K. Szabo, JHEP **1201**, 138 (2012).
 - [10] A. Bazavov *et al.* [HotQCD Collaboration], Phys. Rev. D **86**, 034509 (2012).
 - [11] A. Bazavov, H.-T. Ding, P. Hegde, O. Kaczmarek, F. Karsch, E. Laermann, Y. Maezawa and S. Mukherjee *et al.*, Phys. Rev. Lett. **113**, no. 7, 072001 (2014).
 - [12] S. Borsanyi, Z. Fodor, C. Hoelbling, S. D. Katz, S. Krieg and K. K. Szabo, Phys. Lett. B **730**, 99 (2014).
 - [13] M. Albright, J. Kapusta and C. Young, Phys. Rev. C **90**, no. 2, 024915 (2014).
 - [14] A. Majumder and B. Muller, Phys. Rev. Lett. **105**, 252002 (2010).
 - [15] R. Hagedorn, Nuovo Cim. Suppl. **3**, 147 (1965).
 - [16] R. Hagedorn, CERN yellow report 71-12, (1971).
 - [17] J. Letessier and J. Rafelski, Camb. Monogr. Part. Phys. Nucl. Phys. Cosmol. **18**, 1 (2002).
 - [18] S. C. Frautschi, Phys. Rev. D **3**, 2821 (1971).
 - [19] K. Huang and S. Weinberg, Phys. Rev. Lett. **25**, 895 (1970).
 - [20] J. R. Cudell and K. R. Dienes, Phys. Rev. Lett. **69**, 1324 (1992).
 - [21] K. Johnson and C. B. Thorn, Phys. Rev. D **13**, 1934 (1976).
 - [22] W. Broniowski and W. Florkowski, Phys. Lett. B **490**, 223 (2000).
 - [23] W. Broniowski, W. Florkowski and L. Y. Glozman, Phys. Rev. D **70**, 117503 (2004).
 - [24] K. A. Olive *et al.* [Particle Data Group Collaboration], Chin. Phys. C **38**, 090001 (2014).
 - [25] A. Bazavov *et al.* (HotQCD Collaboration), Phys. Rev. D **85**, 054503 (2012).
 - [26] Y. Aoki *et al.*, JHEP **0906**, 088 (2009).
 - [27] T. Bhattacharya, M. I. Buchoff, N. H. Christ, H.-T. Ding, R. Gupta, C. Jung, F. Karsch and Z. Lin *et al.*, Phys. Rev. Lett. **113**, no. 8, 082001 (2014).
 - [28] Z. Fodor and C. Hoelbling, Rev. Mod. Phys. **84**, 449 (2012).
 - [29] A. Bazavov *et al.* [HotQCD Collaboration], Phys. Rev. D **90**, no. 9, 094503 (2014).
 - [30] M. Cheng, S. Ejiri, P. Hegde, F. Karsch, O. Kaczmarek, E. Laermann, R. D. Mawhinney and C. Miao *et al.*, Phys. Rev. D **81**, 054504 (2010).
 - [31] A. Bazavov *et al.* [HotQCD Collaboration], Phys. Rev. D **86**, 034509 (2012).
 - [32] C. Ratti *et al.* [Wuppertal-Budapest Collaboration], Nucl. Phys. A **855**, 253 (2011).
 - [33] S. Ejiri, C. R. Allton, M. Doring, S. J. Hands, O. Kaczmarek, F. Karsch, E. Laermann and K. Redlich, Nucl. Phys. A **774**, 837 (2006).
 - [34] S. Ejiri, F. Karsch and K. Redlich, Phys. Lett. B **633**, 275 (2006).
 - [35] J. Rafelski, J. Letessier and A. Tounsi, In *Divonne 1994, Hot hadronic matter* 479-492 (1994).
 - [36] K. Redlich and H. Satz, arXiv:1501.07523 [hep-ph].
 - [37] B. Friman, P. M. Lo, M. Marczenko, K. Redlich and C. Sasaki, arXiv:1507.04183 [hep-ph].
 - [38] W. Broniowski, F. Giacosa and V. Begun, arXiv:1506.01260 [nucl-th].